

1 **Simulation of Nanostructures fabricated in chalcogenide**
2 **glasses for use as surface-enhanced Raman**
3 **scattering substrates**

4
5 **A. Zakery^{1,*}, A. Asrar¹, S.R. Elliott²**

6 ¹ *Department of Physics, College of Science, Shiraz University, Shiraz 71454, Iran*

7 ² *Department of Chemistry, Cambridge University, Cambridge CB2 1EW, UK*

8 **Corresponding author: zakeri@susc.ac.ir*

9
10 **Abstract**

11 We have simulated the chalcogenide glass (ChG)-based nanostructures which are used as
12 substrates for surface-enhanced Raman scattering (SERS). A discrete dipole approximation
13 method was used and calculated results are compared to those of experimental. The results of
14 simulation agreed well with the experiment. Furthermore, we have obtained conditions under
15 which higher enhancement factors (almost by an order of magnitude) could be achieved by
16 changing the polarization state and the incident angle of the beam on the surface.

17
18 OCIS codes: 240.6695, 300.6450, 350.4238, 130.3120

19
20 It has been 30 years since it was recognized that the Raman spectra of sub monolayer
21 coverage of molecules could be acquired on electrochemically roughened coinage metal surfaces

22 [1-3]. Since then, the field of surface enhanced Raman spectroscopy (SERS) has grown
23 dramatically, demonstrating its power as an analytical tool for the sensitive and selective
24 detection of molecules adsorbed on noble metal nanostructures.

25 Understanding the mechanisms of SERS has been a struggle since the early days of its inception,
26 when the primary goal was merely explaining the 10^6 -fold intensity enhancement of the normal
27 Raman scattering cross-section. At the time, the enhancement factor, $EF_{\text{SERS}} = 10^6$, could be
28 understood as the product of two contributions: (a) an electromagnetic enhancement mechanism
29 and (b) a chemical enhancement mechanism. These two mechanisms arise because the intensity
30 of Raman scattering is directly proportional to the square of the induced dipole moment, μ_{ind} ,
31 which, in turn, is the product of the Raman polarizability, α , and the magnitude of the incident
32 electromagnetic field, E . As a consequence of exciting the localized surface plasmon resonance
33 (LSPR) of a nanostructured or nanoparticle metal surface, the local electromagnetic field is
34 enhanced by a factor of 10, for example. Because Raman scattering approximately scales as E^4 ,
35 the electromagnetic enhancement factor is of order 10^4 . Researchers viewed the chemical
36 enhancement factor of 10^2 as arising from the excitation of adsorbate localized electronic
37 resonances or metal-to-adsorbate charge-transfer resonances (e.g., resonance Raman scattering).
38 It is also worthwhile to note that surface-enhanced resonance Raman scattering with combined
39 SERS and resonance Raman scattering enhancement factors in the 10^9 – 10^{10} range was possible
40 at the time. Despite this enhancement, which made SERS orders of magnitude more sensitive
41 than normal Raman spectroscopy, the full power of SERS unfortunately was not utilized until
42 this past decade. Early systems suffered immensely from irreproducibility owing to ill-defined
43 substrates fabricated by electrochemical roughening.

44 Recent advances in nanofabrication and the 1997 discovery of single-molecule SERS [4, 5], the
45 ultimate limit of detection, have caused an explosion of new research and the extension of SERS
46 from an interesting physical phenomenon to a robust and effective analytical technique. In
47 addition, surface preparation and modification techniques [6-9] have also allowed for analyte
48 selectivity.

49 The need for new SERS-based sensing, detecting, and monitoring platforms has also
50 driven new instrumental techniques such as the integration of SERS active substrates into fiber-
51 optic assemblies [10]. Su et al. report a new technique in their recent articles [11, 12]. In the first
52 Letter, they presented what they believed to be a new class of SERS substrates based on
53 chalcogenide glasses (ChGs). Owing to their photosensitivity, periodic nanostructures can be
54 easily fabricated in ChG thin films in a convenient and cost effective way. By coating with a thin
55 Au layer, such nanostructures act as effective SERS substrates and are capable of producing
56 detectable Raman signals for low concentrations of analyte molecules. Experiments with
57 aqueous Rhodamine 6G (R6G) solutions were conducted to investigate the behavior of ChG-
58 based nanostructures as SERS substrates. In their work the performance of these SERS substrates
59 is compared with that of silver nanoparticles made using a citrate reduction method. The
60 potential of their SERS substrate for quantitative analysis, as well as its reproducibility, is
61 discussed in some detail. We simulated their experiment using a discrete dipole approximation
62 method and obtained results which will be discussed in further detail.

63 The Discrete dipole approximation [13] (DDA) starts by dividing the object of interest
64 into a cubic array of N -point dipoles whose positions are denoted by r_i , with polarizabilities α_i .
65 The polarization induced in each dipole as a result of interaction with a local electric field E_{loc}
66 will be (omitting the frequency factors $e^{i\omega t}$),

67
$$P_i = \alpha_i \times E_{loc}(r_i) \quad (1)$$

68 $E_{loc}(r_i)$ for isolated particles, is the sum of an incident field and a contribution from all other
 69 dipoles in the same particle,

70
$$E_{loc}(r_i) = E_{loc,i} = E_{inc,i} + E_{self,i} = E_0 \exp(iK \times r_i) - \sum_{i \neq j} A_{ij} \times P_j \quad (2)$$

71 E_0 and K are the amplitude and wave vector of the incident wave, respectively, and the
 72 interaction matrix A has the following form:

73
$$A_{ij} \times P_j = \frac{e^{(iKr_{ij})}}{r_{ij}^3} \left\{ K^2 r_{ij} \times (r_{ij} \times P_j) + \frac{1 - iKr_{ij}}{r_{ij}^2} \times [r_{ij} P_j - 3r_{ij} (r_{ij} \times P_j)] \right\}, (i \neq j) \quad (3)$$

74

75

76 where $K = \omega/c$. Substituting Eq. (2) into Eq. (1) and rearranging terms in the equation, we
 77 generate an equation of the form

78
$$A' \times P = E \quad (4)$$

79 Where A' is a matrix which is built out of the matrix A from Eq. (3). For a system with a total of
 80 N dipoles, E and P in Eq. (4) are $3N$ -dimensional vectors, and A' is a $3N \times 3N$ matrix. By
 81 solving these $3N$ complex linear equations, polarization vectors are obtained, and with these,
 82 optical cross sections, local fields and the Raman enhancement factor can be calculated.

83 As noted earlier we used the DDA for simulating the desired experiments [11]. The
 84 SERS substrate composed of near semicircular dots (with a diameter $d=460$ nm) and intervening
 85 holes as seen in the SEM image. In the atomic force microscope (AFM) image, the semicircular
 86 dots in the SEM images appeared to be hemispheres with a height of 70 nm (see Fig. 1). The
 87 SERS substrate used composed of overlapped hemispheres which produced nanoparticles with a

88 volume of the order of 10^7 (nm)³. It is shown [13] that DDA is suitable for particles of the same
89 order of volume (e. g. spheroids with major axis 200 nm and aspect ratio 2:1).
90 We divided each nanoparticle (each hemisphere) into 2116 cubes where each cube showed one
91 dipole. Because of the rapidly decreasing of EF with distance, practically none of the
92 neighboring cube had a significant effect in our calculations. So we considered only the effect of
93 the first neighboring cube in our calculations. We calculated EF for three different polarizations
94 and eleven different incident angles. We assumed that R6G molecules were distributed
95 uniformly on the surface. For calculation of the number of R6G molecules adsorbed on surface
96 with different concentrations, it is clear that Avogadro's number (A) of molecules exist in one
97 liter of solution in one-molar solution. So $A^{2/3}$ of molecules exist on (10×10) cm² of surface
98 and hence is the calculated number of molecules adsorbed (exist) on our desired surface. DDA
99 method will be more accurate by a correct choice of polarizability α_i in eq. (1) as was used in
100 [14]. Due to a lack of reliable data on dielectric constants of gold nanoparticles of desired size
101 we used dielectric constants of smaller gold nanoparticles which were reported in [15], and
102 obtained good results.

103 In this simulation we obtained $EF=1.478 \times 10^6$ for a vertical incident beam which is one
104 order greater than that of the usual silver nanoparticle substrates [11]. Relative intensities are in
105 good agreement with experimental results [11] (See Figure 2). By choosing the wavenumber
106 position of Raman peaks we found the relative intensity for the two substrates (sers and silver
107 nanoparticle substrates). We calculated the number of R6G molecules on the surface of a
108 nanoparticle. For 1, 10, 50 and 100 μ M we obtained 13, 60, 249 and 390 molecules respectively.
109 In this case intensities are proportional to the number of molecules on each nanoparticle; (see
110 Figure 3). We also calculated EF for 11 different angles equally spaced in range 0- 90° and for

111 different polarizations. A result obtained for three different polarizations is shown in Fig. 4
112 (angles are in radian). Although the state of the polarization was known at the incidence (in the
113 experiment) but its state was not known after passing through various optical elements before
114 being detected. The free space incident beam angle in [12] was 90 degrees. But we obtained
115 conditions that EF can be larger than that reported in [12].

116 For example in Figure 4 for xyz-polarization and incident beam that makes an angle of $\pi/4$ with
117 the surface, the free space EF is five times greater than parallel radiation (with surface) which is
118 like the case of an evanescent wave. So we suggest some situations rather than evanescent wave
119 that give higher EF than that of [12] ; see Figure 4. Relative intensity between evanescent wave
120 and free space wave in [12] is approximately 4/3 which is roughly obtained for x-polarization in
121 our simulations. Other two polarizations do not yield the same result. As seen in Fig. 4, although
122 for x-polarization we have the largest EF for the case of zero angle incidence (evanescent wave),
123 for other polarizations EF is a maximum near $\pi/4$.

124 Some errors in our work are because of (perhaps) inexact dielectric constant of gold
125 nanoparticles. Results with better agreement can be achieved by considering more dipoles in our
126 calculations.

127 In summary, the results of our simulation of chG-based nanostructures compared well
128 with those of experimental. Moreover, we have obtained conditions under which higher
129 enhancement factors (almost by an order of magnitude) could be achieved by changing the
130 polarization state and the incident angle of the beam on the surface. These chG-based substrates
131 are compatible with chG photonic circuits [16] to form integrated SERS sensor chips.

132

133 A. Z would like to thank Shiraz University for a Sabbatical leave.

134
135
136
137
138
139
140
141
142
143
144
145
146
147
148
149
150
151
152
153
154
155
156

Figure Captions

Figure 1: Simulated SERS substrate.

Figure 2: (a) : The top plot is simulated SERS substrate signal and the lower one is simulated Raman spectra of Ag nano particles which correspond to A and B in (b) respectively, (b) : Experimental R6G Raman spectra obtained [11] with A, SERS substrates at 50 mW (0.28 kW/cm²) and 100 μM concentration; B, silver nanoparticles at 500 mW (2.8 kW/cm²) and 1 mM concentration; C, silver nanoparticles at 50 mW (0.28 kW/cm²) and 1mM concentration; D, smooth Au surface at 500 mW (2.8 kW/cm²) and 1 mM concentration.

Figure 3: (a) : Simulation of detected SERS signals for different concentrations of R6G solution, (b) Detected SERS signals at different R6G concentrations with an excitation of 50 mW (0.28 kW/cm²) [11].

Figure 4: (a) : Simulation of Enhancement Factor versus the incident angle for x-polarization; (b) : For yz polarization; (c) : For xyz polarization; (d) Raman spectra obtained [12] with A, fiber-taper-coupled SERS substrate; B, conventional free-space laser-focusing method.

157
158
159
160
161
162
163
164
165
166
167
168
169
170
171
172
173
174
175
176
177
178
179

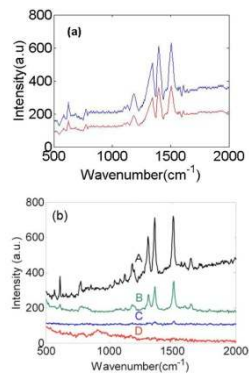
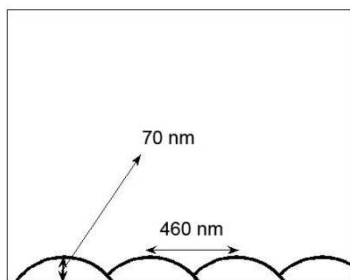
References

1. P.L. Stiles, J.A. Dieringer, N.C. Shah, R.P. Van Duyne, “*Surface enhanced Raman spectroscopy*”, *Annu. Rev. Anal. Chem.* **1**, 601(2008).
2. D.I. Jeanmarie, R.P. Van Duyne, “*Surface Raman spectroelectrochemistry, part 1: heterocyclic, aromatic, and aliphatic amines adsorbed on the anodized silver electrode*”, *J. Electroanal. Chem.* **84**, 1 (1977).
3. M.G. Albrecht, J.A. Creighton, “*Anomalously intense Raman spectra of pyridine at a silver electrode*”, *J. Am. Chem. Soc.* **99**, 5215 (1977).
4. S.M. Nie, S.R. Emery, “*Probing single molecules and single nanoparticles by surface-enhanced Raman scattering*”, *Science* **275**, 1102 (1997).
5. K. Kneipp, Y. Wang, H. Kneipp, L.T. Perelman, I. Itzkan, “*Single molecule detection using surface-enhanced Raman scattering (SERS)*”, *Phys. Rev. Lett.* **78**, 1667 (1997).
6. L.A. Dick, A.D. McFarland, C.L. Haynes, R.P. Van Duyne, “*Metal film over nanosphere (MFON) electrodes for surface-enhanced Raman spectroscopy (SERS): improvements in surface nanostructure stability and suppression of irreversible loss*”, *J. Phys. Chem. B* **106**, 853 (2002).
7. T.R. Jensen, M.D. Malinsky, C.L. Haynes, R.P. Van Duyne, “*Nanosphere lithography: tunable localized surface plasmon resonance spectra of silver nanoparticles*”, *J. Phys. Chem. B* **104**, 10549 (2000).

- 180 8. M.D. Malinsky, K.L. Kelly, G.C. Schatz, R.P. Van Duyne, “*Nanosphere lithography:*
181 *effect of substrate on the localized surface plasmon resonance spectrum of silver*
182 *nanoparticles*”, J. Phys. Chem. **B 105**, 2343 (2001).
- 183 9. X. Zhang, J. Zhao, A. Whitney, J. Elam, R.P. Van Duyne, “*Ultrastable substrates for*
184 *surface-enhanced Raman spectroscopy fabricated by atomic layer deposition: improved*
185 *anthrax biomarker detection*”, J. Am. Chem. Soc. **128**, 10304 (2006).
- 186 10. D.L. Stokes, J.P. Alarie, V. Ananthanarayanan, T. Vo-Dinh, “*Fiber optic SERS sensor*
187 *for environmental monitoring*”, Proc. SPIE **3534**, 647 (1999).
- 188 11. L. Su, C. J. Rowlands, S. R. Elliott, “*Nanostructures fabricated in chalcogenide glass for*
189 *use as surface-enhanced Raman scattering substrates*”, Opt. Lett. **34**, 1645 (2009).
- 190 12. L. Su, C. J. Rowlands, S. R. Elliott, “*Evanescence Wave excitation of surface enhanced*
191 *Raman scattering substrates by optical fiber taper*”, Opt. Lett. **34**, 2685 (2009).
- 192 13. W.-H. Yang, G. C. Schatz, R. P. Van Duyne, “*Discrete dipole approximation for*
193 *calculating optical absorption spectra and surface-enhanced Raman intensities for*
194 *adsorbates on metal nanoparticles with arbitrary shapes*”, J. Chem. Phys. **103**, 869
195 (1995).
- 196 14. B. T. Draine, J. Goodman, “*Beyond Clausius-Mossotti Wave propagation on a*
197 *polarizable point lattice and the discrete dipole approximation*”, Astrophys. J. **405**, 685
198 (1993).
- 199 15. P. Stoller, V. Jacobsen, V. Sandoghdar, “*Measurement of the complex dielectric constant*
200 *of a single gold nanoparticle*”, Opt. Lett. **31**, 2474 (2006).

201 16. V. Ta'eed, M. Shokooh-Saremi, L. Fu, D.J. Moss, M. Rochette. I.C.M. Littler, B.J.
202 Eggleton, Y.L. Ruan and B. Luther-Davies, "*Integrated all-optical pulse regenerator in*
203 *chalcogenide waveguides*", Opt. Lett. **30**, 2900 (2005).
204
205
206
207
208
209
210
211
212
213
214
215
216
217
218
219
220
221

UNDER PEER REVIEW



222

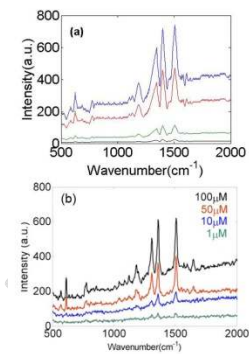
223

224 Fig. 1

225

226

Fig. 2



227

228

229 Fig. 3

230

231

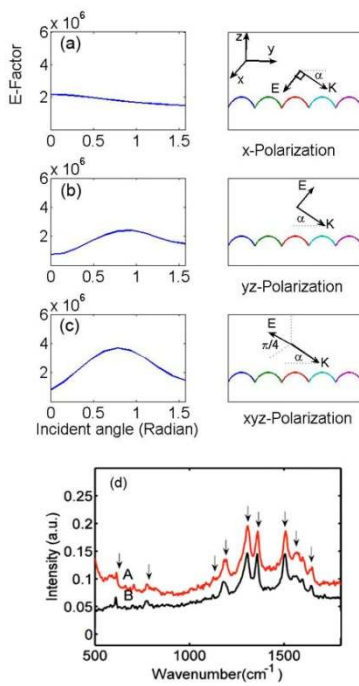


Fig. 4